Estimating Beam Strength of Metallic Gear Materials

Edward E. Osakue
Department of Engineering
Texas Southern University
Houston, Texas,
USA

Lucky Anetor
Department of Engineering
Texas Southern University
Houston, Texas,
USA

Expressions for the pulsating or beam strengths of many popular metallic gear materials are derived based on the tensile strength and endurance ratio. The strength values predicted are for a reliability of 99% at load cycles corresponding to that of the endurance strength of the materials. The expressions are based on the consideration of the revised Lewis gear root stress formula by treating the design parameters as random variables associated with the lognormal probability density function and application of the Gerber fatigue failure rule. Pulsating strength predictions are compared with those of AGMA estimates for through-hardened steels and other materials. The variances between model predictions and AGMA values for steel and ductile cast iron materials are reasonably low. Low variances between model and AGMA values for high-strength gray cast iron and cast bronze were also observed. However, high variances between model and AGMA values for low-strength gray cast iron and cast bronze were found. Overall, the model estimates are considered sufficiently accurate for preliminary design applications where initial sizes of gears are generated. The study showed that for many metallic gear materials, the average pulsating strength ratio is 0.36 at 99% reliability. Therefore, the suggestion by Buckingham, that the fatigue strength of a gear tooth is approximately one-third (0.333) of the tensile strength of the material is justified.

Keywords: *Bending stress, Fatigue, Reliability, Pulsating, Endurance, Failure, Strength*

1. INTRODUCTION

When a component is subjected to load disturbance of a fluctuating nature, fatigue induced failure is a possibility. A tensile stress promotes fatigue failure since a compressive stress tends to close up fatigue cracks. The beam strength of a gear tooth is the maximum stress resistance of the tooth to failure in bending when the loading is uni-directional. It may otherwise, be called pulsating strength due to the unidirectional and repeated loading nature of most gears when in operations. A gear tooth loaded in bending develops maximum tensile stress in the tooth root area. When the tensile stress at the gear root is about equal to the beam strength in value, fatigue crack initiation and growth can occur [1-3].

Fatigue failure occurs in three stages of crack nucleation (initiation) at sites of stress concentration, crack growth or propagation which happens as the repetitive load continues, and finally a sudden fracture, which occurs when the load bearing section of the object is too small to sustain the applied load. Crack nucleation sites are typically at the surfaces or near the surfaces of objects where some form of defects exist. Surface defects such as scratches or pits, sharp corners due to poor design or manufacture, inclusions, grain boundaries, or dislocation concentrations, create nucleation sites. High stress concentrations create plastic strains leading to localized slips that can produce crack initiation. Generally, crack nucleation coincides with the beginning of rapid increase in plastic strain and may happen sometimes well after the loading has started. Crack growth describes the process of gradual increase in the size of a crack and can involve coalescence of multiple micro-cracks and macro-cracks, until fracture occurs. Usually, cracks grow along planes normal to the maximum tensile stress. Fatigue failure is of great concern when metals and polymers are used in the design of objects subjected to repetitive loads [1, 2, 3, 4, 5].

In flaw-free materials, a significant fraction of the total lifetime of a component is spent before the first detectable microcracks appear. At low stress amplitudes, the crack initiation phase can make up a major fraction of the component service life but at high amplitudes, the crack initiation phase is usually a small fraction of the lifetime [6]. Some studies show that crack initiation and propagation to fracture can be simulated numerically, especially with finite element method (FEM). Kastratovic et al. [7] developed an approximate numerical method for estimating a normalized stress intensity factor (SIF) of three co-planar cracks in mode I fracture state in a solid. Grbovic et al. [8] simulated a single surface crack initiation and propagation to fracture of a dental implant. It gives a good understanding of crack formation and growth to failure of a component. The failure mode simulated is typical of components like shafts but may be applicable to gear tooth with modification.

Received: August 2022, Accepted: October 2022
Correspondence to: Edward E. Osakue
Department of Engineering Texas Southern University Houston, Texas, USA
E-mail: edward.osakue@tsu.edu
doi: 10.5937/fme2204587O

Fatigue load cycles may be classified into two groups of finite-life and infinite-life. In finite-life load cycle, a component or product fails at a limited number of load cycles and the stress at failure is called the fatigue strength. Finite-life load cycle is typically in the range of 10^3 to 10^7 load cycles. Infinite-life cycle is generally when a component or product is subjected to 10^6 load cycles and above and the stress at failure is called the endurance strength. Generally, the endurance strength of materials may show little or no decrease with increasing fatigue load cycles in infinite-life fatigue. Most ferrous alloys and titanium exhibit well-defined endurance strength, sometimes well before 10^7 load cycles. Many nonferrous alloys do not exhibit well-defined endurance strength. For materials without apparent endurance strength, it is often taken to be the fatigue strength at 10^8 to 5×10^8 load cycles [9, 10].

The bending strength of gear teeth was first calcu–lated to a reasonable degree of accuracy by Wilfred Lewis in 1892 [4]. He considered a gear tooth as a cantilever beam on a rigid support with the load applied near the tip of the gear. The maximum tensile stress occurs at the root area on the loaded side of the gear tooth. Due to the pulsating loading of a gear tooth, this region becomes the preferential site for the initi–ation of fatigue crack. Gear failure in bending fatigue is one of the common modes of failure [11-13]. Thru-hardened gears most often fail in bending fatigue due to a crack initiated at the surface in the root area. Because the surface hardness of case-hardened gears is higher than the core value, the bending fatigue strength of the gear root surface can be higher than that of the core [14]. Case-hardened gears generally fail in fatigue at the boundary of case-core hardness, except when there is sharp stress raiser at the surface [15]. Several factors may be attributed to bending fatigue failure and include poor gear design, improper assembly, misalignment of gears, overloads, inadvertent stress raisers or subsurface defects, and use of incorrect materials and heat treatments [16].

Aziz et al. [59] indicate that three methods may be used to estimate beam strength of gear materials. These are simple analysis method (SAM), numerical analysis method (NAM), and experimental analysis method (EAM). SAM is based on analytical models developed with simplifying assumptions like the Lewis beam model of gear root bending stress. Application of SAM is fast and needs minimal training and resources. NAM is based on analytical models usually with calculus based formu–lation that often have no close-form solution and finite element method (FEM) is a popular example. Application of NAM can be computationally intensive and slow and needs specialized knowledge and in most cases require considerable computer resources. Both SAM and NAM models may be modified by empirical factors to improve on their performance. EAM uses experimental techniques to determine the beam strength of gear materials. Experimental stress analysis with the use of strain gauges has become widespread [60]. EAM is the most reliable but is very expensive, requires specialized equipment and fundamental knowledge. Also, it is demanding and takes a long for reliable data to be gathered. EAM involves testing samples to failure and may have to be done when new materials need be used for initial design.

It appears that no analytical scientifically based predictive model of beam strength is available. The popular one is that of Buckingham which states that the beam strength is one-third of the tensile strength of a gear material [22]. This is probably informed by experi–mental results and there seems to be no analytical verification for it. If an analytical model is developed so that the beam strength of materials can be estimated from some more easily determined properties like ten–sile strength and or standard fully reversed bending fatigue, initial design of gears may be done with some justifiable confidence, and capacity performance testing can be carried out latter.

The tensile strength of materials is determined experimentally from the tensile test and is relatively simple. Similarly, fully reversed bending fatigue test is much simpler than a gear tooth bending fatigue test, needs less skill, and can have a time duration advantage. Estimating gear tooth beam strength from a less costly and less time-consuming test will eliminate initial experimentations for gear beam strength determination, speed up product development, and reduce product cost. It must be noted though, that the shape of standard specimens in tensile and fully reversed bending fatigue testing experiments is not the same as that of gear tooth which is a part of larger component. Also, a fully reversed fatigue specimen is usually smoothly polished, while the root area of a gear tooth may have machining and grinding marks, tear marks, rough finish, or corrosion [17]. Therefore, the need for actual load capacity determination of a gearset after it is built by testing is obvious.

The objective of this study is the formulation of a scientific and sound engineering approach for esti–mating the beam strength of a gear tooth from the tensile strength and endurance ratio of the gear material for preliminary gear design at 99% reliability. As stated earlier, when the tensile stress at the gear root is about equal to the beam strength, fatigue crack initiation and growth can occur. If a gear tooth is sized such that the maximum tensile stress at the root area is less than the beam strength, bending fatigue failure at the root may be avoided or a reasonable gear service life may be achieved. Since current estimates of beam strength are mainly empirical, it will be helpful and useful to have a reliable and scientifically based estimation method for it. This study provides some answers in that direction.

2. SPUR GEAR EQUIVALENCE OF HELICAL GEAR

A spur gear has teeth parallel to the shaft axis while a helical gear has teeth inclined at an angle to the shaft axis. The angle of inclination of a helical gear to the shaft axis is called the nominal helix angle. Cylindrical gears consist of spur and helical gears and a spur gear is a special type of a helical gear with a nominal helix angle of 0^o. Generally, the nominal helix angles of helical gears vary from 5° to 50°. The nominal helix angles for single-helical gears fall between 5° and 25° and those for double-helical gears fall between 20° and 45°. The nomi–nal helix angle is selected so as to obtain a minimum overlap ratio that ensures good load sharing [17-20].

A spur gear has transverse and axial planes associated with it. The transverse plane is the plane of rotation and is perpendicular to the axial plane. The gear diameter is defined on the transverse plane and the gear facewidth is defined on the axial plane. Helical gears have a normal plane in addition to axial and transverse planes and the tooth profile is defined on the normal plane. The shape of a helical gear in the normal plane is almost exactly the same as that of a spur gear with a larger number of teeth [17]. In a spur gear, the normal and transverse planes are coincident. Like spur gears, the driving force in helical gears lies in the transverse plane but actual contact of gear teeth occurs in different plane. Therefore, the operation of a helical gearset depends on what happens on the contact plane.

The equivalent spur gear for a helical gear has the same load capacity as the helical gear. The two parameters which relate a helical gear to its equivalent spur gear are the transverse pressure angle and the base helix angle [19]. When the normal pressure angle is standardized for helical gears, then:

$$\phi_t = \tan^{-1}\left[\frac{\tan\phi_n}{\cos\psi}\right] \quad \psi_b = \tan^{-1}\left[\tan\psi\cos\phi_t\right] \qquad (1)$$

Equation (1) contains two expressions and should be interpreted as Eq. (1a) and Eq. (1b) from left to right. The same rule should be applied to other equations of similar nature.

According to Maitra [18], the base helix angle (Eq. (1b)), gives a more accurate estimate of the radius of curvature of an equivalent spur gear. Consequently; it may be used to define a plane, called the virtual plane, for a helical gear where an equivalent or virtual spur gear may the analyzed. The virtual spur gear has a larger number of teeth than the actual helical gear. The analysis of an equivalent spur gear is simpler than the actual helical gear and its pitch diameter is obtained as the basic spur gear diameter divided by the square of the cosine of the base helix angle [19].

3. GEAR FATIGUE LOADING AND MAXIMUM ROOT BENDING STRESS

Most gear teeth are loaded only in *one direction (*uni-directional*)* during operation, but some gears such as idler gears, planetary pinions and gears used in reversing mechanisms are loaded in *both directions* (bi-directional) [14, 21]. Components that are loaded in both directions are said to be in fully reversed fatigue while those loaded in one direction are said to be in pulsating fatigue [22]. In one directional loading, the load rises from zero value to a maximum value and drops back to zero value. This loading pattern is repeated rhythmically in the operation of a gearset and is also called pulsating loading. A bi-directional loading creates a loading pattern of maximum positive load and maximum negative (minimum) load. In fully reversed fatigue loading, the absolute values of maximum and minimum loads are equal. Both uni- and bi-directional loading is repeated once per revolution, leading to dynamic fluctuations in load values.

Fig. 1 depicts the two types of gear tooth loading, with Fig. 1a representing pulsating loading and Fig. 1b, representing fully reversed loading. For *infinite life* design, peak stresses must be below the *pulsating or endurance strength* in bending for the gear materials, depending on the loading type. In *finite life design*, peak stresses must be below the fatigue strength, which depends on the expected load cycles in bending for the gear material for either pulsating or fully reversed fatigue.

Fig. 1a: Pulsating bending load

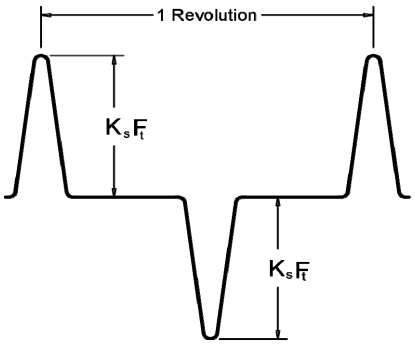

Fig. 1b: Fully reversed bending load

In Fig. 1, the design load is indicated as the product of the service load factor and the nominal transmitted load that can be obtained from Eq. (2).

$$F_t = \frac{2T\times10^3}{d} \qquad T = \frac{30P\times10^3}{\pi N} \qquad (2)$$

The design problem of a gear tooth loaded in bending fatigue requires the evaluation of the fluctu–ating maximum tensile stress at the tooth root area and ensuring that it is less than the fatigue strength of the material at that point. A fillet is usually provided at the gear tooth root area that creates some stress concen–tration, making it the critical point for fatigue crack initiation.

Osakue & Anetor [23, 24] formulated a reversed Lewis beam strength capacity model for cylindrical gears which apply to gear meshes with multiple pairs of contacts. The expression for this design capacity model on the virtual plane defined by the base helix angle is:

$$\sigma_t = \frac{2K_s k_\sigma k_t T\times10^3}{\lambda_e \varpi_v m_n b d Y_v} \le S_t \qquad (3)$$

The parameters T, b, d, N, k^t, $Y_v^|$, S_t in Eqs. (2) and (3) apply to either the pinion or gear in a mesh. Separate equations for the pinion or gear may be obtained by appending subscript 1 for the pinion or 2 for the gear, respectively to these parameters. In Eq. (3) the value of the stress concentration factor k_σ is independent of the load point on the gear tooth during operation. For materials permeated with internal discontinuities like

cast irons, stress raisers usually have little effect, regardless of loading because surface or geometric dis–continuities seldom cause more severe stress concent–ration than that already associated with internal disc–ontinuities. However, for most engineering materials like steels and polymers, stress concentration should be considered when there is fatigue or impact loading [21].

The original Lewis bending stress form factor Y_v is for gears without addendum modification. But the trend in the gear industry is the increasing use of addendum modified gears in power transmission for better performance [18, 25]. In addendum modified gears, equivalent value of Y_v has to be evaluated and used. Note that Y_v and ϖ_v in Eq. (3) are based on the virtual number of teeth z_v of gears [19] given in Eq. (4b), not the actual number of gear teeth.

$$Y_v = f\left(z_v\right) \quad z_v = \frac{z}{\cos^3{}_b} \tag{4}$$

4. GERBER FATIGUE FAILURE AND PULSATING STRENGTH

Failure under dynamic load is most often of the fatigue type and about 80-90% of failures from mechanical and structural elements are due to fatigue. According to Norton [26], three approaches are generally used in fatigue design. These are the stress-life (*S-N*) approach, the strain-life (ε-*N*) approach, and the linear elastic fracture mechanics (LEFM) approach. The *S-N* fatigue design approach is currently the most popular for high-cycle fatigue design where the expected load cycles are more than about 10^3 [26], which is typical of most gear drives. In this approach, the damage from cyclic bending stress state is assessed on the basis of the mean and amplitude stresses for one load cycle. The exact variation of the stress during the cycle does not seem to be particularly relevant [27, 28]. When a tensile mean stress is present during a fatigue load cycle, the material can fail at amplitude stress level lower than the fatigue strength. Among popular models addressing this problem are the Gerber, Goodman, and Soderberg [9]. The Gerber yield criterion is a better approximation to fatigue failure in the presence of tensile mean stress [29] and represents average behavior of ductile materials accurately [26]. Because the Gerber fatigue failure model represents average behavior of ductile materials [26, 30], it may be associated with 50% reliability in design. This is attract–ive because fatigue strengths are usually determined at 50% reliability and therefore, represents a very good fit [9, 10]. In the case of cumulative fatigue damage, the Miner's rule is the most commonly used failure theory.

In fatigue loading, the maximum stress in a load cycle is:

$$S_{\max} = S_m + S_a \tag{5}$$

Most gear teeth experience pulsating stress cycle for which:

$$S_m = S_a = 0.5 S_{\max} \tag{6}$$

The Gerber failure rule for a uniform strength probability of 50% failure rate is given in Eq. (7).

$$\frac{S_a}{S_e^*} + \left[\frac{S_m}{S_{ut}^*}\right]^2 = 1 \tag{7}$$

Please, note that Eq. (7) above is a slightly modified version of the conventional Gerber fatigue failure rule. Conventionally, S_e^* is replaced, with S_e which is obtain–ned at 50% reliability [40, p. 157] while S_{ut}^* is replaced with S_{ut} which is obtained at 99% reliability [30]. Therefore, there is an obvious mismatch of reliability values in the conventional application of the Gerber fatigue failure rule. For consistency in applying the Gerber fatigue failure rule, a correction factor is required to convert S_{ut} value at 99% reliability to that at 50% reliability. To that effect, it is assumed that the Eq. (8a) can be established.

$$S_{ut}^* = k_o S_{ut} \qquad S_e^* = \alpha_e S_{ut} \tag{8}$$

The parameter k_0 is the ratio of mean tensile strength to minimum tensile strength and has a value greater than unity. An expression for k_o is provided in Appendix A9. Note that k_0 is only required when minimum tensile strength value is known. If strength data are mean values, k_0 assumes a value of unity. The bending endurance strength of a material is related to its tensile strength by the endurance ratio as in Eq. (8b). The endurance ratio α_e, is less than unity in value.

Substitute Eq. (6) into Eq. (7) to obtain Eq. (9).

$$S_a = \frac{S_{ut}^{*2}}{2S_e^*}\left[\sqrt{1+4\left(\frac{S_e^*}{S_{ut}^*}\right)}-1\right] \tag{9}$$

Based on Eq. (5), the pulsating strength is obtained as expressed in Eq. (10).

$$S_0^* = \frac{S_{ut}^{*2}}{2S_e^*}\left[\sqrt{1+4\left(\frac{S_e^*}{S_{ut}^*}\right)^2}-1\right] = S_{\max} \tag{10}$$

When Eq, (8a) is substituted in Eq. (10), then:

$$S_o^* = \frac{k_o^2 S_{ut}^2}{S_e^*}\left\{\sqrt{1+4\left(\frac{S_e^*}{k_o S_{ut}}\right)^2} - 1\right\} \tag{11}$$

If experimental values of S_{ut}, k_0, and S_e^* are avai–lable, Eq. (11) directly gives estimate of S_o^*. This will be the most accurate estimate that can be obtained of the basic pulsating strength without direct experimental measurement. However, in preliminary design situa–tions, it may be that only the tensile strength and endu–rance ratio for the material type are available. In this situation, Eq. (8b) can be substituted in Eq. (11) to obtain Eq. (12).

$$S_0^* = \frac{k_0^2 S_{ut}}{\alpha_e}\left\{\sqrt{1+4\left[\frac{\alpha_e}{k_0}\right]^2}-1\right\} \tag{12}$$

Eq. (12) may be used also to obtain an accurate estimate of S_o^*, but the endurance ratio α_e and mean strength factor k_0 must be evaluated from experimental values. When experimental value of S_e^* is unavailable, but approximate values of α_e and k_0 are available, as might be the case during preliminary design, then Eq. (12) can be used to estimate S_o^* in an "approximate" sense. Therefore, Eq. (11) may be regarded as the "accurate" model for S_o^*, while Eq. (12) is the "appro–ximate" model.

Eq. (12) can be transformed into Eq. (13) to define a pulsating strength ratio, which is similar to the endurance ratio. That is:

$$S_o^* = \alpha_o S_{ut} \qquad \alpha_o = \frac{k_o^2}{\alpha_e}\left\{\sqrt{1+4\left[\frac{\alpha_e}{k_o}\right]^2} - 1\right\} \tag{13}$$

Eq. (13a) provides an expression for the basic pulsating strength of a material based on the Gerber fatigue rule. The value estimated is an average value at 50% reliability.

As an example, consider steel materials for which $\alpha_e = 0.50$ and $k_o = 1.152$ from Table A2 in Appendix A5. Substitution in Eq. (13b) leads to:

$$\alpha_o = \frac{1.152^2}{0.5}\left\{\sqrt{1+4\times\left(\frac{0.5}{1.152}\right)^2} - 1\right\} = 0.8605$$

Hence from Eq. (13a):

$$S_o^* = 0.8605 S_{ut} \tag{14}$$

Eq. (14) is the specific expression for the pulsating strength of steel materials at 50% reliability. A similar expression can be obtained for any other material if α_e and k_0 can be estimated.

5. NOMINAL STRENGTHS OF GEAR MATERIALS

The basic endurance and pulsating strengths above need to account for the variability of design parameters, strength properties, and reliability other than 50% for practical usefulness. A generic nominal design factor is defined and evaluated probabilistically and then applied to the basic strengths to obtain the nominal endurance and pulsating strengths of gear materials at 99%. These are expressed, respectively in Eq. (15a) and (15b).

$$S_o^{/} = \beta_o S_{ut} \qquad S_e^{/} = \beta_e S_{ut} \tag{15}$$

where:

$$\beta_o = \frac{\alpha_o}{n_o} \qquad \beta_e = \frac{\alpha_e}{n_e} \tag{16}$$

Eqs. (15) and (16) can be applied in specific and generic senses. If values of β_o and β_e are obtained from data for specific materials like steel, cast iron or bronze, Eq. (15) will yield an expression specific to that material type. If values of β_o and β_e are obtained from the combined data of different materials like steel, cast iron and bronze, then Eq. (15) will yield a generic expression for those set of materials. The generic expressions are:

$$S_o^{/} = \varpi_o S_{ut} \qquad S_e^{/} = \varpi_e S_{ut} \tag{17}$$

In Eq. (17), a single value of ϖ_o or ϖ_e applies to different types of materials in a data set of their evaluation. Therefore, estimates from Eq. (17) are not as reliable as those from Eq. (15).

5.1 Nominal Probabilistic Design Factor

A lognormal probabilistic design factor model has been proposed [31] for many design situations. The model considers design parameters as random variables and characterizes them with a mean value and a coefficient of variation (cov). The cov of each design parameter is estimated using sensitivity analysis of the first order Taylor's series expansion. The model is surprisingly simple because it is a function of only two parameters: the reliability parameter (z_0) and the variability parameter (s_m). The reliability parameter is the same as the unit normal variate and defines the level of risk acceptable in a design task through a reliability target. The variability parameter is the lognormal standard deviation of the assumed lognormal probability density function. It combines all the significant variability and uncertainty which are quantified by covs in a design capacity model into one parameter value. The reliability and variability parameters define the nominal reliability factor for a specific design.

The lognormal model [31] has been applied in the re-design of different types of components and com–parison with previous results showed very good to ex–cellent agreement. These include the design of a tension bar and crane girder [32], design of a bolt and flange joint [33], design of a cyclically loaded cantilever beam [28], contact strength estimate [34, 41], and design of shafts for bending and torsion [35]. Because the nominal design factor is probabilistically evaluated, it transforms conventional deterministic design equations into reliability-based design when used in deterministic design equations.

The lognormal standard deviation associated with a design capacity model due to the variability of the design parameters may be estimated as [31]:

$$s_m = \sqrt{\ln\left[\left(1+\vartheta_M^2\right)\left(1+\vartheta_S^2\right)\right]} \tag{18}$$

The nominal design factor n_0 based on z_0 and s_m is estimated as [31]:

$$n_o = \exp\left[s_m(z_o + 0.5 s_m)\right] \tag{19}$$

American Society for Testing Metals (ASTM) specifies minimum strength at a reliability of 99% with a corresponding unit normal variate of $z_0 = 2.326$.

As an application of Eq. (18) and Eq. (19), consider steel gears with $\vartheta_M = 0.293$, from Appendix A1, and $\vartheta_S = 0.115$ from Appendix A5, Table A3. When these values are substituted in Eq. (18):

$$s_m = \sqrt{In\left[(1+0.293^2)(1+0.115^2)\right]} = 0.309$$

From Eq. (19), for $z_0 = 2.326$:

$$n_o = \exp\left[0.309(2.326 + 0.5 \times 0.309)\right] = 2.152$$

From Eq. (16a) and Eq. (15a), we then have:

$$\beta_o = \frac{\alpha_o}{n_o} = \frac{0.8605}{2.152} = 0.40 \quad S_o^{/} = 0.40 S_{ut} \tag{20}$$

For steels, the tensile strength is related to the hardness as in Eq. (21a) [41] and Eq. (20b) becomes Eq. (21b) for through-hardened steel gears:

$$S_{ut} = 3.269 H_s \quad S_o^{/} = 1.3076 H_s \tag{21}$$

For case-hardened steel gears, the core hardness is used to replace the surface hardness of through-hardened gears.

5.2 Service Pulsating and Endurance Strengths

The service pulsating or endurance strength of a component like a gear tooth is different from that of a specimen used in an experiment in a laboratory due to several reasons. For instance, the specimen is tested in the laboratory while the gear may be used in the field in closed or open gearbox. The shape and size of a gear tooth will usually be different from that of a standard specimen used in the laboratory. Therefore, it is necessary to have some adjustment in order to obtain realistic estimate of endurance or pulsating strength for gear components by modifying the nominal strength with an effective correction factor as indicated in Eq. (22).

$$S_o = S_o^{/} Y_f \qquad S_e = S_e^{/} Y_f \tag{22}$$

The effective correction factor is obtained from Eq. (23a) when surface roughness is unaccounted for or from Eq. (23b), when surface roughness is accounted for.

$$Y_f = Y_n Y_r Y_s Y_z \qquad Y_f = Y_n Y_r Y_z \tag{23}$$

The bending durability, reliability and size factors are defined in American Gear Manufacturers Asso–ciation (AGMA) standards and methods of evaluations are provided. A temperature factor is included in some versions of AGMA standards. However, if gear teeth operate in an elevated temperature, the fatigue and tensile strength properties of the material at that temperature should be used [21]. This will give a more realistic estimate of strength; therefore, a temperature factor is omitted in Eq. (23).

Tests on specimens with varying surface roughness values have shown that fatigue cracks always occur at the most pronounced surface flaw or roughness [36]. Gear root areas are commonly left as machined surfaces due to possible residual tensile stress that grinding can produce. Another possible reason for leaving gear root area machined is that grinding the area is rather difficult [56]. Shigley and Mischke have suggested an expo–nential relationship for surface roughness factor based on the experimental data of Noll and Lipson [22] for steels. The surface finish factor for machined surface is given by Eq. (24a) from [30]. When Eq. (21a) is substituted in Eq. (24a), the result is Eq. (24b).

$$Y_s = 4.45 S_{ut}^{-0.265} \le 1.0 \quad Y_s = 3.251 H_s^{-0.265} \le 1.0 \tag{24}$$

For case-hardened steel gears, the surface finish factor Y_s is unity when tooth failure is expected in the core, not at the surface. For steel materials that may fail from surface cracks, when account is taken of surface roughness, Eq. (24b) is applied to Eq. (21b) to give the nominal strength of through-hardened steel gears in Eq. (25a) and that of case-hardened steel gears in Eq. (25b).

$$S_o^{/} = 4.251 H_s^{0.735} \qquad S_o^{/} = 1.3076 H_c \tag{25}$$

AGMA specifies grade 1, grade 2, and grade 3 quality levels for steel gear materials. Grade 2 and grade 3 materials have higher beam strengths than grade 1. Available gear strength data from AGMA are generated from tests on actual gears [26] and empirical expression for the beam strength of through-hardened steel gear materials in the hardness range of 190 to 425 HVN [14] is provided. For grade 1 through-hardened steel gears; the nominal pulsating strength is:

$$S_o^{/} = 0.5052 H_c + 83.3 \tag{26}$$

Because the strength estimate of Eq. (26) is based on actual experimental data, it is inherently corrected for surface finish effects and perhaps to some extent, stress concentration effects.

6. ESTIMATES OF GEAR BEAM STRENGTH

The equations presented in the previous sections were coded in Microsoft Excel for computational efficiency. The goal was to estimate the beam strengths of some metallic gear materials using the new formulas and make comparisons with those from AGMA. AGMA standards are perhaps the most popular gear standards in use and have a good reputation amongst gear designers and manufacturers. In Appendix A5, data on bending pulsating and endurance ratios and covs are summarized from different sources for several common gear materials and values of the variability parameter (s_m) were determined. Then values of β_0 and β_e were evaluated at $z_0 = 2.326$ for 99% reliability by subs–titution of data values into Eqs. (13), (15), 16, and (17). The nominal design factors for approximate pulsating strength (Eq. (12)) and the accurate pulsating strength (Eq. (11)) models, respectively, were determined. Similarly, the nominal design factor for approximate endurance strength was evaluated. Table 1 is a summary of the values of β_0 and β_e obtained. They are extracts from Table A3 and Table A4, respectively from the Appendix.

In order to validate beam strength predictions from the formulated models, comparisons with published strength data are made. Beam strength data have been determined by AGMA [26] for different types of gear materials and data for steel materials appear more common as steel is the most popular gear material. Steel

materials may be thru-hardened or case-hardened to improve performance. Thru-hardening processes can produce hardness in the range of 150 – 500 HVN with higher values obtained for alloy steels than for plain carbon steels. The core and surface hardness are approximately the same for thru-hardened steels. Case-hardening is used when surface hardness of about 450 HVN and above is desired [37] and it gives core hardness substantially lower than the surface hardness. The commercially acceptable tolerance range for surface hardness is about 30 to 50 HVN, with 40 HVN being common [24].

Table 1: Fatigue Ratios of Some Materials

Material	99% Reliability	
	β_0	β_e
GCI*	0.366	0.207
DCI*	0.341	0.191
CGI*	0.371	0.211
ADI*	0.315	0.175
Cast steel	0.368	0.210
Copper alloys	0.310	0.174
Nickel alloys	0.348	0.197
Steel and alloys	0.400	0.236
Titanium alloys	0.425	0.254
Aluminum	0.336	0.187
Magnesium	0.300	0.164
Average	0.359 (ϖ_o)	0.206 (ϖ_e)
*GCI-Gray cast iron; DCI-Ductile cast iron; CGI-Compacted graphite iron; AGI-Austempered ductile iron		

Comparisons of nominal pulsating strength predictions from models of Eq. (15) and Eq. (25) with AGMA values for different metallic gear materials are provided in Table 2 to Table 5. Table 2 shows comparisons of nominal pulsating strengths from AGMA and the models for through-hardened steel materials, based on Eq. (25) and Eq. (26). Table 3 shows comparisons of strength values for ductile cast iron with model values based on Eq. (15a) and Eq. (17a). Similarly, Table 4 shows comparisons of strength values for gray cast iron, and Table 5 shows comparisons of strength values for cast bronze materials. Available beam strength data in public domain for other materials are not as plentiful as for steel materials. Specifically, available beam strength data for non-ferrous gear materials are scarce.

Table 2: Nominal Bending Strength Estimate

Comparison for Grade 1 Steel Materials

Surface Hardness (HVN)	Nominal Bending Strength (MPa)			Variance (%)	
	AGMA	Model-Spec.	Model-Gen.	Spec.	Gen.
150	164	169	152	2.92	-7.39
200	189	209	188	10.19	-0.74
250	215	246	221	14.54	3.18
300	240	281	253	17.18	5.56
350	265	315	284	18.73	6.96
400	290	347	313	19.58	7.72
450	316	379	341	19.96	8.06
Model-Spec./Gen.= Specific model/Generic model					

Table 3: Nominal Bending Strength Estimate Comparison for Ductile Cast Iron Materials

Minimum Tensile Strength (ksi)	Nominal Bending Strength (MPa)			Variance (%)	
	AGMA	Model-Spec.	Model-Gen.	Spec.	Gen.
80	190	188	199	-1.00	4.51
100	230	235	248	2.23	7.92
120	260	282	298	8.52	14.56

Table 4: Nominal Bending Strength Estimate Comparison for Gray Cast Iron Materials

Minimum Tensile Strength (ksi)	Nominal Bending Strength (MPa)			Variance (%)	
	AGMA	*Model-Spec.*	*Model-Gen.*	*Spec.*	*Gen.*
20	35	51	50	45.71	41.84
30	59	76	74	28.32	26.21
40	90	101	99	12.16	10.32

Table 5: Nominal Bending Strength Estimate Comparison for Bronze Material

Minimum Tensile Strength (ksi)	Nominal Bending Strength (MPa)			Variance (%)	
	AGMA	Model-Spec.	Model-Gen.	Spec.	Gen.
40	39	86	99	120.5	153.8
90	163	192	223	17.8	37.0

7. DISCUSSIONS

Table 2 to Table 5, show model estimates based on the data in Table 1 and AGMA strength data. In these tables, two predicted model values are provided. The first set of values is the specific model (Model Spec.) values and the second set is the generic model (Model Gen.) values. Eqs. (25) and (26) were used for model strength estimates for steel materials. For non-steel materials, the Model-Spec. estimates in the tables are from Eq. (15a) with values of β_0 taken from Table 1 for the different materials. For the Model-Gen. estimates, the value of ϖ_o = 0.36 in Eq. (17a) and was taken from the last row of column 2 in Table 1. The variance in each table is the percentage difference between AGMA and model predicted values. The AGMA values in these tables are used as reference values for comparison because of the global acceptability of AGMA standards in gear technology. In Tables 2 to 5, the variances in column 5 are based on the comparison of the specific model values with AGMA values. Similarly, in the tables, the variances in column 6 are the based on the comparison of the generic model values with AGMA values.

Table 2 compares pulsating strength values from both the specific and generic models with AGMA values for steel materials. The variances in columns 5 of Table 2 are in the range of 2.92 to 19.96% and the positive variance values indicate that the model values are slightly higher than AGMA values. The variances in column 6 for the generic model values are from - 7.39 to 8.06%. The generic model appears to indicate a better match with AGMA values than the specific model because the generic fatigue ratio of 0.36 is lower than the specific value of 0.4. Correction was made for

surface roughness for steel materials since AGMA data are based on tests of actual gears with surface roughness. The values of the variances in Table 2 would have been much higher without correction for surface roughness for the steel materials. Steel materials are usually sensitive to stress concentration effects [21], and surface roughness can be very influential in determining fatigue strength. The specific model estimates are deemed more accurate in this table because AGMA models are said to be conservative [55].

Table 3 compares pulsating strength values from both the specific and generic models with AGMA val–ues for ductile cast iron. The variances in Table 3 are quite low; being in the range of -1.0% to 8.52% for the specific model values and 4.51 to 14.56% for the gene–ric model. The higher variance values for the generic model are due to the strength ratio of 0.341 for the specific model being smaller than 0.360 for the generic model. The sample size is rather low, though compa–rison results are favorable. It should be noted that no surface finish adjustment was made for ductile cast iron. Internal flaws in cast irons make the materials largely insensitive to stress concentration effects, hence surface finish would not dramatically influence fatigue strength.

Table 4 compares pulsating strength values from both the specific and generic models with AGMA values for gray cast iron. The generic model shows a marginal improvement over the specific model values because the generic fatigue ratio is 0.36 while the specific fatigue ratio is 0.366. According to Mott [11], pulsating strength of cast iron is about 0.35 times the tensile strength. The comparison between the pulsating ratio estimate of 0.366 and 0.35 is excellent as the difference is only 4.6%. The variances in Table 4 appear generally high but lower for higher tensile strengths than low tensile strength. Again, the sample size is small, and generalization based on it can only be a crude approximation.

Table 5 compares pulsating strength values from both the specific and generic models with AGMA values for cast bronze. The variances in Table 5 for higher strength cast bronze are considerably lower than the lower strength type. However, it appears that the specific model estimate is fairly good for the material of high strength grade of the bronze materials. Like cast iron, surface finish adjustment was not made for copper alloys. Copper and its alloys are quite ductile and ductile materials generally have low sensitivity to stress concentration effects. Hence, surface roughness is expected to have marginal or no effect on the fatigue strength predictions.

7.1 Low-Strength Gray Cast Iron and Bronze

As noted above, the pulsating fatigue strength estimates from the derived formulas for low-strength gray cast iron and cast bronze are significantly higher than AGMA recommended values. Since the estimates for other types of materials and for the higher strengths of these materials seem reasonable, it may well be that the AGMA recommended values are rather conservative in these cases. To explore this idea, consider Table 7 where the pulsating strengths are estimated directly from the tensile and endurance strengths of the materials obtained from [38] using Eq. (11) and shown in column 4 of Table 7. The design factors in columns 5 and 6 are average values for the complete dataset evaluated in Appendix A5. Strength values in column 7 are obtained by dividing values in column 3 by design factor in column 5. Similarly, strength values in column 8 are obtained by dividing values in column 4 by design factor in column 6. The values of pulsating strengths in column 4 and column 8 of Table 7 are considered the most accurate at the indicated reliability levels because they are based on experimental data of the tensile and endurance strengths of the materials.

Table 7: Pulsating Strength Based on Experimental Tensile and Endurance Strengths

Material	Strengths at 50% Reliability (MPa)			Design Factors at 99% Reliability		Strengths at 99% Reliability (MPa)	
	Tensile	Endurance	Pulsating	Endurance	Pulsating	Endurance	Pulsating
Gray cast iron	152	69	124	2.19	2.40	32	52
Bronze-sand cast	305	170	288	2.19	2.40	78	120

Table 8: Comparison of Pulsating Strength Estimates

	Pulsating Strengths at 99% Reliability (MPa)			Deviations (%)	
Material	Accurate Model	Approx. Model	AGMA	Approx. Model	AGMA
Gray cast iron	52	51	35	-1.92	-32.70
Bronze-sand cast	120	94	39	-21.67	-67.50

Table 9a: Pulsating Strengths from Other Sources with endurance strength factor of 70%

Material	Pulsating Strength (MPa)				Endurance Strength (MPa)		
	Other Sources			AGMA	Other Sources		
Gray cast iron	55	56 [58]	55 [55]	35	38.4 [44]	38.5	38.4
Bronze-sand cast	108	99	122 [22]	39	75 [21]	69 [39]	85

Table 9b: Pulsating Strengths from Other Sources with endurance strength factor of 63%

Material	Pulsating Strength (MPa)				Endurance Strength (MPa)		
	Other Sources			AGMA	Other Sources		
Gray cast iron	61	56 [58]	55 [55]	35	38.4 [44]	35	35
Bronze-sand cast	119	110	122 [22]	39	75 [21]	69 [39]	77

Table 8 shows a comparison of the approximate model and AGMA values with the accurate model estimates which are based on experimental data of Table 7. Both the approximate model and AGMA values are lower than the accurate model estimates. However, the AGMA values show higher deviations from the accurate model estimates from values in columns 5 and 6 of Table 8, respectively. As mentioned earlier, the AGMA values in these low-strength cases seem rather conservative. This opinion appears to be reinforced when data from other sources on these materials are considered as may be deduced from the discussion below.

The endurance strength of cast iron (170 HVN) is reported as 84 MPa [40, p. 1042]. Endurance strength data are obtained as average data which can be associated with 50% reliability. The 84 MPa value becomes 38.4 MPa at 99% reliability when the endurance strength design factor of 2.19 in Table 7 is applied. AGMA recommends that endurance strength is about 70% of pulsating strength [14, p. 800]. The corresponding pulsating strength at 99% reliability would be 55 MPa for the cast iron material. Khurmi & Gupta [58, p. 1039] quote pulsating strength of ordinary cast iron as 56 MPa, while Gope [40, p. 889] quotes a value 55 MPa. The above estimates and quoted values are quite consistent but considerably higher than AGMA value of 35 MPa.

The endurance strength of phosphor bronze worm gear (SAE 65) is usually taken as 165 MPa [21]. At 99% reliability, the 165 MPa value becomes 75 MPa when the endurance strength design factor of 2.19 in Table 7 is applied. The corresponding pulsating beam strength at 99% reliability would be 108 MPa. A different source says the endurance strength of bronze is 69 MPa [39], which gives 99 MPa as pulsating strength. According to Bhandari [22], the pulsating strength of bronze may be estimated as 40% of tensile strength which gives 122 MPa for the material in Table 7. This gives 85 MPa as endurance strength for the bronze material at 99% reliability.

Table 9a gives a summary of the pulsating and endurance strength data from other sources. Values of endurance strengths in Table 9a are taken as 70% of the pulsating strength values where the former is known and the later unknown. The known values are referenced in the table. Similarly, pulsating strength values are taken as the endurance strength values divided by 70%. In Appendix A6, it is shown that basic endurance strength is about 63% of basic pulsating strength on the average. This ratio translates to a better match between pulsating strength values in Table 9b and the estimate in Table 7 from the numbers in the last two rows of columns 2 and 3 of Table 8 and last two rows of Table 9b.

When AGMA beam strength values in Table 9a are compared with estimates from other sources, considerable differences are observed. For instance, the AGMA beam strength value for cast iron is at least 36.4% lower and that for cast bronze is at least 60.6% lower than those of other sources. In Table 9b, the AGMA beam strength value is at least 36.4% lower for cast iron and 64.5% lower for cast bronze than those from other sources. Consequently, the AGMA beam strength values appear to be quite conservative for low-strength values of cast iron and cast bronze materials. Therefore, the variances in the model values for these materials in Table 4 and Table 5 for low strength materials, respectively; may be considered as outliners.

The "accurate" model (Eq. 11) estimate of beam strength for the cast iron in Table 7 is 52 MPa and the average value in Table 9b is 57 MPa from other sources. The deviation of the accurate model estimate from the average value is -9.3%, the negative value being indicative a conservative prediction. Similarly, the "accurate" model estimate of the beam strength for the cast bronze in Table 7 is 120 MPa and the average value from other sources in Table 9b is 117 MPa. The model prediction deviates from the average value by 2.6%, which is apparently an excellent estimate. Therefore, the beam strength data of Table 9b appear to validate the "accurate" model of Eq. (11), though, indirectly. The same argument may be made for Table 9a. This is very reassuring and the accurate model appears reliable.

The analysis in the study for the "approximate" model assumes that the working data are the endurance ratio and the tensile strength of the gear material. In the "accurate" model, it is assumed that experimental values of tensile strength and endurance strength of the material are available. Because the tensile strength is evaluated at 99% reliability, the resulting nominal pulsating ratio and endurance ratio are defined at 99% reliability also. The 99% reliability is the default for both AGMA [63] and International Standardization Organization (ISO) [64] gear design standards. Adjustment for other reliability levels can be made by the use of reliability factor. Based on the lognormal probability density function assumed in the study, values of the reliability factor have been evaluated. Table A5 gives values of the reliability factor for some reliability levels.

Endurance strength is usually associated with a number of load cycles. The load cycles for the endurance strength for magnesium, copper and nickel alloys are 10^8 and 10^7 for titanium. That for aluminum is 5×10^8 load cycles [13] and it is 3×10^6 load cycles for steels. The predicted strength values by the models correspond to the load cycles of the material endurance strength, except when modified by the durability and other factors based on expected service conditions.

7.2 Practical Relevance of Study

The endurance strength of a gear tooth is influenced by material type, loading (reversed or pulsating), surface finish, size of tooth, and stress concentration at gear root [22]. In practice, it is difficult to know the specific contributions of these factors for each and every gear design [22]. However, gear sizing and adequacy assessment cannot be done without knowledge of endurance or beam strength. By combining statistics, probability, and fatigue failure theories; the authors have developed models that can predict the beam strength of metallic materials using easily determined strength properties.

Currently, estimates of beam strength for initial sizing of gears in design applications are based on

empirical relations. The most popular is that of Buckingham that states that the beam strength is about one-third (0.333) of the tensile strength of the gear material [22]. This appears to have held up well till date but no analytical proof seems to be available. But empirical expressions are developed after expensive experimentation and data analysis. From Table 1, the average pulsating strength ratio for the metallic materials shown is 0.36 at 99% reliability. The work presented in this paper clearly demonstrates analytically, the reasonableness of Buckingham's statement and shows that 99% reliability may be associated with the estimate. This verification seems to be a worthy theoretical contribution to gear science and technology.

According to National Broach & Machine, the fatigue strength of gear teeth follows a statistical pattern, necessitating the use of a safety or design factor [61]. Impact loads in gear systems are commonly two or more times the rated load. As a general rule, when peak loads exceed twice the rated load, it is necessary to consider yield failure in both material selection and design [61]. The nominal design factor for the approximate model of Eq. (13) or Eq. (15) in the paper is evaluated to be 2.23 and 2.19 for endurance strength of Eq. (16). It is estimated to be 2.4 for the more accurate model of Eq. (11). The design factor estimates from the study seem to be within practically known load ranges in gear systems. Thus, it appears that adequate consideration was given to load and material variability by the authors in the developed models to assure realistic beam strength estimates for metallic gear materials. This is quite comforting and attests to the practical relevance of the study.

Due to rapid development in material science, more and more materials are being put forward by researchers [62]. The behavior of new materials is often not known very well and available design properties are not often complete. This is especially true of gear beam strength which takes considerable time to obtain results. The models presented are most valuable when new materials with limited design data such as tensile strength and endurance strength are available. Tensile strength is obtained from a tensile test which is relatively inexpensive, fast and reliable. Now, reasonable estimate of endurance strength can be made from the material tensile strength just by identifying the material family even for newly developed materials through the endurance ratio. Therefore Eq. (12) or Eq. (13) of the paper becomes very relevant in such situations. Rather than build gears with the new materials and test them to failure, tensile and perhaps endurance strength tests may be done, and the beam strength estimate from these equations used to perform initial gear sizing. The verification and validation phases of design can then be conducted latter to confirm or improve on design results and preliminary reliability.

Though the beam strength models formulated are based on design parameter variability and uncertainty of cylindrical gear root stress model of Eq. (3), they are also applicable to other gear types of the involute form. Helical gears have a normal plane which is defined by the nominal helix angle. Other involute gears such as bevel, face, and worm gears, are likewise defined in the normal plane [65]. Therefore, when these other gear types are converted to their equivalent spur gears, they are similar to the equivalent spur gear of a helical gear. Now, the loading and stressing of these other gear types are similar to those of cylindrical gears. Also, the load variability and material strength variability are of the same nature and roughly of the same magnitudes. Furthermore, the parameter Y_v in Eq. (3) is purely a geometric parameter. The parameter k_0 is independent of gear shape and point of load application on the gear tooth in a mesh which distinguishes it from the gear root bending stress models of AGMA [63] and ISO [64]. It is a property of the gear material and fillet size at the gear root. Consequently, the results of the study for pulsating and endurance strengths are still valid for these other gear types. Hence, estimates of beam strength by the formulated models for the materials considered may be used for all gear types.

There appears to be some confusion about pulsating and endurance strengths of gear tooth in the literature since the two appear to be referred to as simply "fatigue strength". Specifically, endurance strength is the stress capability for two-way or fully reversed bending fatigue, while pulsating strength is the stress capability for one-way bending fatigue (please refer to Fig. 1). Fully reversed bending fatigue involves a stress reversal from positive to negative but pulsating bending fatigue does not. It varies from zero value to a maximum and then the pattern is repeated in every load cycle. Hopefully, this study should bring some clarity to the differences between bending endurance strength and pulsating strength and aid better communications in this area of gear technology.

Accurate estimates of gear stresses are difficult to obtain due to uncertainty about values of stress concentration factor, residual stresses, external and internal dynamic overloads, etc. Therefore, the best way to find out how much load a gearset will carry is to build and test it. However, very good guesses can now be made due to research in gear design technology and the use of advanced modeling tools such as (FEM) [17]. But, FEM needs initial geometry, which is why a reasonably accurate analytical model for preliminary sizing of gear components becomes very important. A good estimate of the beam strength of a gear material is of immerse relevance in the initial sizing of gears when experimental data are unavailable. When the beam strength estimate can be obtained from a fast, reliable and easily performed experiment like tensile test, it speeds up the design process and minimizes product developmental costs. The models developed in this study are most useful in this regard.

7.3 Design Adequacy Assessment

Since the estimation of the gear root bending stress is not exact, gear loads in service and fatigue strength have a statistical nature; it is practically impossible to completely eliminate the probability of fatigue failure in gear design [57]. The probabilistic approach used in the study is very significant in this regard. It allows gear design reliability to be interpreted in "safety" terms based on desired failure rate. Due to the uncertainty

mentioned, it is reasonable to allow for unknown factors in design practice that could cause premature failure [14]. Therefore, an apparent design factor may be introduced in assessing gear design adequacy. Consequently, in a design application, it may be required for pulsating strength resistance that:

$$n_t = \frac{S_o}{\sigma_t} \geq n_\# \qquad S_t = \frac{S_o}{n_\#} \tag{27}$$

And for endurance strength resistance that:

$$n_t = \frac{S_e}{\sigma_t} \geq n_\# \qquad S_t = \frac{S_e}{n_\#} \tag{28}$$

Because most of the variability and uncertainty in relevant design parameters and factors are already accounted for in n_o, a modest value of $n_\#$ should suffice [11]. $n_\#$ may be prescribed by standards or codes or agreed on with a client which must be adhered to. For instance, from Table 2 to Table 5; except for the low strength gray cast iron and cast bronze, which are considered as exceptions, the maximum variance between the model estimates and AGMA values is mostly below 20 % for the specific model. Consequently, $n_\#$ =1.25 is perhaps reasonable for initial sizing. According to Petrov et al. [42], the apparent design factor for contact stress may be increased by 15% for critical gear drives. Therefore, the minimum apparent design factor for bending endurance may be increased by about 30% for critical gear drives against bending stress failure.

The nominal design factor is 2.156 at 99% reliability from Table A3 for steel materials. From [41], the average design factor for steel material with respect to contact stress is 1.502. The square of 1.502 is 2.256, which deviates from 2.156 by -4.64%, indicating a very close match. This should not be a surprise since bending stress is directly proportional to load and the contact stress is proportional to the square root of load.

Gear tooth fractures due to bending generally start in the root fillet area. Occasionally, a new tooth may break as a result of severe overload or serious defect in the tooth structure. Gear failure by tooth breakage is usually a fracture induced slow progressive failure and often happens in a brittle manner. Pitting and scoffing may weaken the tooth before it breaks. High load resistance against breakage at the gear tooth root may be achieved by using large module, large root fillet, quench-tempered or case-hardened materials, and a positive profile shift for gears with small number of teeth [43]. Compressive stresses can enhance fatigue resistance, so manufacturing processes such as shot peening, proof loading, carburizing, nitriding, and induction hardening are used in gear processing. These processes induce residual compressive stresses on the surfaces of the parts so treated, thus mitigating the deleterious effects of tensile stresses on the parts [44] that can cause fatigue failure.

8. CONCLUSIONS

A probabilistic design factor approach is combined with the Gerber fatigue rule and the revised Lewis gear root bending stress model in developing expressions for the pulsating strength of gear materials. The probabilistic approach treats design parameters as random variables associated with the lognormal probability density function or can be approximated by it. The design parameters are characterized by a mean value and coefficient of variation (cov). The variability of design parameters in the revised Lewis stress model is analyzed and with a desired reliability level, a probabilistic nominal design factor is quantified. The nominal design factor is applied to the Gerber fatigue failure rule to establish gear material nominal beam strength models. The expected life of the gear tooth in load cycles corresponds to that of the endurance strength of the gear material. Model predictions are at 50% and 99% levels but values at 99% reliability are preferred for a reasonable service

Two models are presented in Eq. (11), the "accurate" model and Eq. (12), the "approximate" model. They are modified by design factors in Eq. (15) and Eq. (16). The "approximate" beam strength model is based on the tensile strength and endurance ratio of the gear material. The "accurate" beam strength model is based on experimental values for both tensile and endurance strengths. Beam strength predictions from Eqs. (15) and (25) are compared in Table 2 with those of AGMA estimates (Eq. (26)) for steel materials. The variances in columns 5 of Table 2 range from 2.92 to 19.96% for the specific model values. The positive variance values indicate that the model estimates are slightly higher than AGMA values. The variances in the generic model are more favorable for steel materials. Comparisons of model predictions and AGMA estimates for ductile cast iron are favorable in Table 3, where the variances are from -1.0 to 8.52 % for the specific model and from 4.51 to 14.56% for the generic model. Good comparisons are obtained for high-strength gray cast iron and cast bronze materials. However, results for low-strength gray cast iron and cast bronze do no indicate favorable comparison with AGMA values. However, it is demonstrated in the study that the AGMA strength recommendations for low-strength gray cast iron and cast bronze materials are perhaps conservative. Overall, the deviations of model estimates from AGMA values are not unreasonable.

The study showed that for many metallic materials, the average pulsating strength ratio is 0.36 at 99% reliability. Therefore, the suggestion by Buckingham [22], that the endurance strength of gear tooth is approximately one-third of the tensile strength of the material is justified and may be associated with 99% reliability. Also, the study suggests that the endurance strength is about 63% of the pulsating strength of gear materials at 99% reliability. Furthermore, the models suggest a nominal design factor of 2.19 and 2.40 for the "approximate" and "accurate' beam strength estimates, respectively at 99% reliability. Adjustments for other probability values are provided in Table A5.

The model estimates seem sufficiently accurate for preliminary gear design applications. The specific model is recommended for the materials listed in Table 1 while the generic model may be used only for metals not listed in the table. The favorable comparisons of model predicted beam strength values with AGMA data sug–

gest that reasonable beam strength predictive models based on sound scientific and engineering analysis have been developed.

ACKNOWLEDGEMENTS

This study was supported with funds and resources from the College of Science, Engineering, and Technology (COSET) Research Fund and the University Faculty Development Fund of Texas Southern University, Houston, Texas. The authors are very grateful for this support.

NOMENCLATURE

ADI – austempered ductile iron
CGI – compacted graphite iron
DCI– ductile cast iron
GCI– gray cast iron
HVN – hardness: Vicker's number
COV – coefficient of variation
cov – coefficient of variation
1, 2 – subscript for bodies in contact
b – nominal facewidth of gear (mm)
F_t – tangential force (N)
T – transmitted torque (Nm)
d – pitch diameter of gear (mm)
H_s – surface hardness (HVN)
H_c – core hardness (HVN)
k_o – mean strength factor
k_{oe} – mean strength factor for basic endurance strength
k_{op} – mean strength factor for basic pulsating strength
k_t – stress combination factor
K_a – application factor
K_i – internal dynamic load factor
K_s – service load factor
N – rotational speed(rpm)
m_n – normal module
n_e – nominal endurance design factor at 99% reliability
n_o – nominal pulsating design factor at 99% reliability
$n_{\#}$ – minimum apparent design factor
n_t – apparent fatigue design factor
P – transmitted power (W)
S_a – alternating stress
S_m – mean or steady stress
$S_{\max}$ – maximum stress in fatigue load cycle
S_e^* – basic endurance strength at 50% reliability
S_o^* – basic pulsating strength at 50% reliability
$S_e^{/}$ – nominal endurance strength at 99% reliability
$S_o^{/}$ – nominal bending pulsating strength at 99% reliability
S_e – service endurance strength at 99% reliability
S_o – service pulsating strength at 99% reliability
S_f – fatigue beam strength
S_{ut} – ultimate tensile strength
Y – generic variable
Y_v – modified Lewis stress factor for virtual gear teeth
Y_t – transformed Lewis stress factor
Y_f – effective bending fatigue strength factor
Y_n – bending durability factor
Y_r – bending reliability factor
Y_s – surface finish factor
Y_z – size factor for bending fatigue
z – actual number of gear teeth
z_v – virtual number of gear teeth
Z – generic variable
k_σ – normal stress concentration factor
k_τ – shear or tangential stress concentration factor
λ_o – basic endurance strength factor
ϕ_t – transverse pressure angle
ϕ_n – normal pressure angle
ψ – nominal helix angle
ψ_b – base helix angle
σ_t – gear root tensile stress
λ_e – effective gear facewidth factor
ϖ_v – virtual plane contact ratio
β_o – specific nominal pulsating strength factor at 99% reliability
β_e – specific nominal endurance strength factor at 99% reliability
ϖ_e – generic nominal pulsating strength factor at 99% reliability
ϖ_o – generic nominal endurance strength factor at 99% reliability
α_e – endurance strength ratio at 50% reliability
α_o – pulsating strength ratio at 50% reliability
λ_e – effective facewidth factor
μ_M – adjusted design capacity model mean
μ_s – combined correlation coefficient mean
μ_t – basic design capacity model mean
ϑ_{ks} – cov of K_s
ϑ_b – cov of b
ϑ_{mc} – miscellaneous cov
ϑ_{ka} – cov of K_a

ϑ_{ki} – cov of K_i

ϑ_{ms} – cov for general miscellaneous variability

ϑ_{ma} – cov for design capacity model accuracy

ϑ_{ut} – cov for ultimate tensile strength

ϑ_{υ} – cov for Poisson's ratio

ϑ_{mf} – cov for failure model correlation coefficient

ϑ_{mh} – cov for human factor variability

$\vartheta_{\mu t}$ – cov of basic design capacity model

$\vartheta_{\mu c}$ – cov of correlation coefficients

ϑ_{Yt} – cov of Y_v and k_t combined

ϑ_{yf} – cov of effective bending fatigue strength factor

ϑ_{yn} – cov for load cycles

ϑ_{yr} – cov for reliability factor

ϑ_{ys} – cov for surface finish factor

ϑ_{yz} – cov for size factor

ϑ_{ko} – cov for mean strength factor

ϑ_{so} – cov for basic approximate pulsating strength

ϑ_{C} – cov for service approximate pulsating strength

ϑ_{O} – cov for basic accurate pulsating strength

ϑ_{OC} – cov for service accurate pulsating strength

ϑ_{se} – cov for basic approximate endurance strength

ϑ_{S} – cov for service approximate endurance strength

ϑ_{M} – effective cov for design capacity model

ϑ_{Y} – cov of Y

ϑ_{Yv} – cov of Y_v

ϑ_{z} – cov of Z

REFERENCES

[1] Chang, K-H, *Product Performance Evaluation Using CAD/CAE*, Academic Press, Elsivier, New York, 2013, Chap. 4.

[2] Askeland, D. R. and Phule, P. P., (2003), *The Science and Engineering of Materials*, 4th Ed., Thomson, Brooks/Cole, United States.

[3] Polasik, S. J., Williams, J. J., Chawla, N. Narasimhan, K. S., *Fatigue Crack Initiation and Propagation in Ferrous Powder Metallurgy Alloys*, Advances in Powder Metallurgy and Particulate Materials, p. 2042 – 2056, May, 2001.

[4] Bommisetty, V. S. N. K, *Finite Element Analysis of Spur Gear Set*, Masters' Thesis, Mechanical Engineering Department, Cleveland State University, 2012.

[5] Šraml M. and Flašker, J., (2007), Computational Approach To Contact Fatigue Damage Initiation Analysis Of Gear Teeth Flanks, Int J Adv Manuf Technol, (2007) 31:1066–1075; DOI 10.1007 /s00170-005-0296-2

[6] Deng, G.J., Tu, S.T., Zhang, X.C., Wang, Q.Q., Qin, C.H., (2015), *Grain size effect on the small fatigue crack initiation and growth mechanisms of nickel-based superalloy,* GH4169, Eng. Fract. Mech. 134, 433–450.

[7] Kastratovic, G., Vidanovic, N., Grbovic, A., and Rasuo, B., *Approximate Determination of Stress Intensity Factor for Multiple Surface Cracks*, FME Transactions (2018), 46, 39 – 45.

[8] Grbovic, A. M., Rasuo, B. P., Vidanovic, N. D., and Peric, M. M., *Simulation of Crack Propagation in Titanium Mini Dental Implants (MDI)*, FME Transactions (2011), 39, 165 – 170.

[9] Osakue, E. E., Anetor, L. and Odetunde, C., A *Generalized Linearized Gerber Fatigue Model*, Machine Design, Vol. 4, ISSN 1821-1259, p. 1-10, 2012.

[10] Osakue, E. E., *A Linearized Gerber Fatigue Model*, International Journal of Modern Engineering, Vol. 12, No 1, p. 64 - 72, 2012.

[11] Mott, R. L. *Machine Elements in Mechanical Design*, 4th ed. SI, Pearson Prentice Hall, New York. 2004.

[12] Bergseth, E. *Influence of Gear Surface Roughness, Lubricant Viscosity and Quality Level on ISO 6336 Calculation of Surface Durability*, Technical Report, Department of Machine Design, Royal Institute of Technology, Stockholm, https://www.diva-portal.org/smash/get/diva2:489751/FULLTEXT01.pdf, 2009.

[13] Schmid, S. R., Hamrock, B. J. and Jacobson,B. O., *Fundamentals of Machine Elements*, 3rd ed., CRC Press, New York, 2014.

[14] Budynas, R. G. and Nissbett, J. K., *Shigley's Mechanical Engineering Design*, 9th ed., McGraw Hill Education, Delhi, 2010.

[15] Dobrovolsky, Zablonsky, K., Mak, S., Radchik, A., and Erlikh, L. *Machine Elements*, Foreign Language Pub. House, Moscow, 1965.

[16] Metals Handbook, 8th Edition. Volume 10: *Failure Analysis & Prevention*, 1975.

[17] Dudley, D. W. (2009), *Handbook of Practical Gear Design*, CRC Press, Boca Raton.

[18] Maitra, G. M., (2013), *Fundamentals of Toothed Gearing*: Handbook of Gear Design, 2nd ed., McGraw Hill, New Delhi.

[19] Osakue, E. E. and Anetor, L., *Helical Gear Contact Fatigue Design By Spur Gear Equivalency*, Int'l Journal of Research in Engineering and Technology, Vol. 06, Issue 02, 2017

[20] Meherwan P. Boyce, *in Gas Turbine Engineering Handbook* (Fourth Edition), 2012

[21] Juvinall, R. C. and Marshek, K. M. Juvinall's *Fundamentals of Machine Component Design*, S.I. Version, Wiley, Singapore, 2017.

[22] Bhandari, V. B. *Design of Machine Elements*, 3rd ed., McGraw-Hill Education, New Delhi.

[23] Edward E. Osakue and Anetor, L*., Revised Lewis Bending Stress Capacity Model for Cylindrical Gears*, The Open Mechanical Engineering Journal, 2020, Vol. 14, pp. 3 - 16.

[24] Edward E. Osakue, Anetor, L. and Harris, K., A *Parametric Study of Frictional Load Influence in Spur Gear Bending Resistance*, FME Transactions journal, (2020) 48, 294 - 306

[25] KHK, *Calculations of Gear Dimensions* https://khkgears.net/new/gear_knowledge/gear_technical_reference/calculation_gear_dimensions.html, Kohara Gear Industry Co., Ltd., Saitama-ken, 332-0022, Japan.

[26] Norton, R. L. (2000), *Machine Design: An Integrated Approach*, Prentice-Hall, Upper Saddle River, New Jersey, Chap. 7.

[27] Kravchenko, P. Y. E. (1964). *Fatigue Resistance*. New York: Pergamon

[28] Osakue, E. E., *Probabilistic Design with Gerber Fatigue Model*, Mechanical Engineering Research, Vol. 1, p. 99 -117, doi:10.5539/mer.v3n1p99, 2013.

[29] Orthwein, W., *Machine Component Design*, West Pub. Coy., New York, 1990, p. 189

[30] J. E. Shigley & C. R. Mischke (Chief Editors), *Standard Handbook of Machine Design*. New York: McGraw-Hill.

[31] Osakue, E. E. and Anetor, L, *A Method for Estimating a Probabilistic Design Factor*, Int'l Journal of Research in Engineering and Technology, Vol. 06, Issue 08, pp. 119 – 129, 2017.

[32] Osakue, E. E. and Anetor, L., *A Lognormal Reliability Design Model*, Int'l Journal of Research in Engineering and Technology, Vol. 5, Is. 7, pp. 245 – 259, 2016.

[33] Edward E. Osakue, Lucky Anetor, Christopher Odetunde, *Reliability-Based Component Design*, Proceedings of ASME 2015 International Mechanical Engineering Congress & Exposition, IMECE2015, November 13-19, 2015, Houston, Texas, USA

[34] Edward E. Osakue, Anetor, L. and Harris, K., *Pitting Strength Estimate for Cast Iron and Copper Alloy Materials*, FME Transactions (2021) 49, 269-279; doi:10.5937/fme2102269O.

[35] Osakue, E. E*., Probabilistic Fatigue Design of Shaft for Bending and Torsion*, Int'l Journal of Research in Engineering and Technology, Vol. 3, Is. 9, p. 370 – 386, DOI: 10.15623/ijret.2014.0309059, 2014

[36] Chermilevsky, D, Lavrona, E, & Romano, V., *Mechanics for Engineers*, MIR Pub., Moscow, 1984, p. 373

[37] Osakue, E. E. and Anetor, L., *Helical Gear Bending Fatigue Desig*n, Int'l Journal of Research in Engineering and Technology, Vol. 06, Issue 04, 2017.

[38] *ASTM Class 20 Standard Gray Iron Test Bars, as Cast & Tin Bronze UNS90700 Sand Castings* http://www.matweb.com/search/datasheet.aspx?

[39] Boston Gear, *Engineering Information: Spur Gears*; https://www.bostongear.com/-/media/Files/Literature/Brand/boston-gear/catalogs/p-1930-bg-sections/p-1930-bg_engineering-info-spur-gears.ashx

[40] Gope, P. C., *Machine Design: Fundamentals and Applications*, PHI Learning Private Ltd. Delhi, 2012,

[41] Edward E. Osakue, Anetor, L. and Harris, K., An *Estimate of the Pitting Strength of Steel Materials*, FME Transactions (2021) 49, 1 -120; doi: 10.5937/fme2101001O.

[42] Chernilevsky, D., Berezovsky, Y. & Petrov, M., *Machine Design*, MIR, Moscow, 1988.

[43] *Chapter 7: Spur Gear Pair Calculation According to DIN 3990 and Other Standards*; https://www.eassistant.eu/fileadmin/dokumente/eassistant/etc/HTMLHandbuch/en/eAssistantHandb_HTML_ench7.html

[44] Rortbart, H. A. & Brown, T. H. (2006), *Mechanical Design Handbook*, 2nd ed., McGraw-Hill, New York, p.5.34.

[45] *Helix Angle Tolerance*; https://www.practicalmachinist.com/vb/general/crossed-helical-gears-helix-angle-tolerance-309404/

[46] Chernilevsky, (1990), *Practical Course in Machine Design*, MIR, Moscow, p. 67.

[47] *Technical Data*; https://www.kggear.co.jp/en/wp-content/themes/bizvektor-global-edition/pdf/TechnicalData_KGSTOCKGEARS.pdf

[48] Osakue, E. E*., Lognormal Reliability-Based Component Design*, Technical report, Department of Industrial Technology, Texas Southern University, Houston, Texas, U.S.A, 2015.

[49] Roshetov, D., Ivanov, A., and Fadeev, V., *Reliability of Machines*, MIR, Moscow, 1990.

[50] Ashby, M. F. and Jones, D. R. H., (1986), *Engineering Materials 2: An Introduction to Microstructures*, Processing and Design, Pergamon Press, Oxford, p. 267

[51] Ullman, G. D, Appendix C: *The Statistical Factor of Safety, The Mechanical Design Process*, 2nd ed., McGraw-Hill, New York, 2009.

[52] *Ductile Iron*; https://www.ductile.org/didata/Section3/3part1.htm

[53] *Compacted Graphite Iron-Mechanical and Physical Properties for Engine Design*, SinterCast, - Supermetal CGI- https://www.sintercast.com/media/1686/sintercast-cgi-mechanical-and-physical-properties-for-engine-design-1.pdf

[54] Zanardi, F., *Fatigue Properties and Machinability of ADI*, Fonderia; http://www.aimnet.it/allpdf/pdf_pubbli/10_05/Zanardi.pdf.

[55] Childs, P. R. N., *Mechanical Design Engineering Handbook*, Butterworth Heinemann Elsevier, Boston, 2014.

[56] Koutsis, A. Common Gear Failures, Gearsolutions .com, June, 2017.

[57] Introduction and Perspectives, https://www. Asminternational.org/documents/

[58] Khurmi, R. S. & Gupta, J. K., A Textbook of Machine Design, S. Chand Technical, 2008.

[59] Aziz, I. A. A., Idris, D., M. N., Mohd, W., *Investigating Bending Strength of Spur Gear: A Review*, MATEC Web Conference, 90, 01037 (2017), DOI: 10.1051/matecconf/20179001037.

[60] Irsel, G., *Bevel Gear Strength Calculations: Comparison of ISO, AGMA, DIN, KISSsoft and FEM Methods*, Journal of the Chinese Society of Mechanical Engineers, Vol. 42, No. 3, pp. 315 – 323, 2021.

[61] National Broach & Machine, *Back to Basics: Material Selection and Heat Treatment*, Gear Technology, July/August, 1985, 40 – 47.

[62] \Surnis, P., & Kulkarni, P., *Material Selection for Spur Gear Design Using Ashby Chart*, Int'l Research Journal of Engineering and Technology, Vol. 7, Is. 9, 2020, p. 62 -72.

[63] American Gear Manufacturers Association, 2004, Fundamental Rating Factors and Calculation Methods for Involute Spur and Helical Gear Teeth, ANSI/AGMA 2004-D04.

[64] ISO 6336-3:2006-09, Calculation of Load Capacity of Spur and Helical Gears -- Part 3: Calculation of Tooth Bending Strength.

[65] Kapelevich, A., *Direct Gear Design*, CRC Press, Boca Raton, New York.

APPENDIX A: SIMPLIFIED RELIABILITY BASED DESIGN ANALYSIS

A1: Design Capacity Model Variability

The basic design or stress capacity model of Eq. (3) needs to be adjusted for analytical accuracy, failure mode correlation with mechanical capability, and human related variability. This could be done by use of coefficients as suggested by [41] in Eq. (A1a).

$$\mu_M = \mu_c \times \mu_t \qquad \vartheta_M = \sqrt{\vartheta_{\mu c}^2 + \vartheta_{\mu t}^2 + \vartheta_{mc}^2} \tag{A1}$$

Eq. (A1b) is an expression for the coefficient of variation (cov) of the adjusted design capacity model expressed by Eq. (A1a). The cov of each design parameter is estimated using sensitivity analysis of the first order Taylor's series expansion [31 - 40]. Usually, there are approximations in data modeling and estimation uncertainty is unavoidable in most situations. Consequently, a miscellaneous cov may be associated with the model of Eq. (A1a) as indicated in Eq. (A1b).

The analysis and estimations in the sections below provided values of $\vartheta_{\mu s}$ = 0.132 from Appendix A2, $\vartheta_{\mu t}$ = 02565from Appendix A3, and ϑ_{mc} = 0.05 is assumed. Hence, substituting values in Eq. (A1b):

$$\vartheta_M = \sqrt{0.132^2 + 0.2565^2 + 0.05^2} = 0.293$$

A2: Correlation Parameters Variability

The correlation parameters on the basic stress capacity model are indicated in Eq. (A2a) and the associated cov expression is given by Eq. (A2b).

$$\mu_c = k_{ma} k_{mf} k_{mh} \qquad \vartheta_{\mu c} = \sqrt{\vartheta_{ma}^2 + \vartheta_{mf}^2 + \vartheta_{mh}^2} \tag{A2}$$

For the design of gears, model accuracy cov, ϑ_{ma} = 0.05 and human related variability in gear design rep–resents a cov ϑ_{mh} of about 0.07 [24]. Assume cov ϑ_{mf} = 0.10 for fatigue failures based on Gerber rule. Substituting values in Eq. (A2b):

$$\vartheta_{\mu c} = \sqrt{0.05^2 + 0.1^2 + 0.07^2} = 0.132$$

A3: Basic Stress Capacity Model Variability

Eq. (A3a) is a reproduction of Eq. (3) with a slight modification.

$$\mu_t = \frac{2K_s k_\sigma T \times 10^3}{\lambda_e \varpi_v m_n b d Y_t} \tag{A3a}$$

The stress capacity model variability of Eq. (A3a) is expressed in Eq. (A3b).

$$\vartheta_{\mu t} = \sqrt{\vartheta_{ks}^2 + \vartheta_{k\sigma}^2 + \vartheta_{Yt}^2 + \vartheta_{\varpi t}^2 + \vartheta_{mn}^2 + \vartheta_b^2 + \vartheta_d^2} \tag{A3b}$$

The parameter K_s accounts for increases and variations in the nominal or rated load due to acceleration and deceleration of connected external and internal masses in a device, tolerances in components in an assembly and the rigidity of supporting structures. It may be expressed as:

$$K_s = K_a K_i \qquad \vartheta_{ks} = \sqrt{\vartheta_{ka}^2 + \vartheta_{ki}^2} \tag{A4}$$

The values of ϑ_{ka} is in the range of 0.05 to 0.20 [48] and the values of ϑ_{ki} is in the range of 0.10 to 0.15 [49]. Generally, higher external load variation in a device during operation will induce higher internal load variation. Thus, the possibility of both the external and internal load variations being at maximum values simultaneously is real but likely remote. Therefore ϑ_{ka} = 0.20 and ϑ_{ki} = 0.10 will be assumed in this analysis.

$$\vartheta_{ks} = \sqrt{0.20^2 + 0.10^2} = 0.224$$

The expressions for Y_t in Eq. (A3a) and its cov are given in Eq. (A5a) and Eq. (A5b), respectively.

$$Y_t = \frac{k_t}{Y_v} \qquad \vartheta_{Yt} = \sqrt{\vartheta_{Yv}^2 + \vartheta_{kt}^2} \tag{A5}$$

Simplified variability analysis of k_t is presented in Appendix 9 from which ϑ_{Yt}= 0.05, approximately.

Variations in component geometry are controlled by manufacturing practices and they are generally small, especially in mating components which is of the order of 0.001 [30] for cross-sectional dimensions in machine design. Gear diameters are mating components and are

accurately manufactured, so ϑ_d = 0.001 is assumed. Gear module is accurately controlled too during manufac–turing and ϑ_{mn} = 0.001 is assumed. Manufacturing control of gear facewidth is not as critical as its diameter and ϑ_b = 0.01 is assumed. The other cov values are ϑ_{ks} = 0.224, ϑ_{Yt} = 0.05 from above, $\vartheta_{\varpi t}$ = 0.03 is assumed, and $\vartheta_{k\sigma}$ = 0.11 [30]. Substituting values in Eq. (A3b):

$$\vartheta_{\mu t} = \sqrt{0.224^2 + 0.11^2 + 0.05^2 + 0.01^2 + 2\times 0.001^2 + 0.03^2} = 0.2565$$

A4 Fatigue Strength Variability and Analysis

A4.1 Strength Variability Considerations

There is ample evidence of the variability of mechanical properties of materials. The mechanical strength of ductile materials do not vary much so a few tests can help determine the properties with good confidence. Strength data for brittle materials generally show more variability [29] and they always have a wide scatter in strength, especially those without ductility [50]. Therefore, many tests are required to accurately determine the strength properties and the property distributions of brittle materials. Variations in mechanical strengths may be attributed to internal cracks and flaws, air holes in steels, cavities in welds, foreign inclusions in the materials and quality of production. Blanks for part making can be of castings and wrought (forged, extruded, rolled, drawn, stamped) materials, or of welded fabrications. Cast metals have large numbers of voids in their lattices that can compromise strength in tension [50]. Wrought products are generally more refined in structure than cast products. Welded fabrications, like cast iron products comp–romising inclusions and heat affected zone effects.

There is always some uncertainty as to the corres–pondence of the properties of test specimens with those of actual parts. Mechanical strengths vary along bar length and among products from different suppliers. If specimen(s) are cut from the same blank or workpiece from which a part is made, the portion used as speci–men(s) is different from the portion of the part. The fact that the specimens may not be from the same portion of the blanks or workpieces from which the parts are made from suggests that complete identicality cannot be assured. Variations in manufacturing process in the same facility between batches and in different facilities lead to variations in strengths of samples and products.

A practical way to characterize variability of nume–rical quantities is to specify the mean value and the cov. The cov is the ratio of standard deviation to the mean of a sample. The cov of tensile strength for wrought steel is about 0.06 [30, 48]. Dobrovolsky et al. [15] assumed that undetected defects may reduce strength by 5 – 10% in forged parts, while they may reduce strength by 15 – 20% in cast parts. Thus, forged products may have a cov of about 3% (0.03) to 4% (0.04). Cast products may exhibit up to about 10% reduction of strength relative to forged or wrought products. That is a cov of about 3% to 4% increase in variability. For cast copper alloy and cast-iron materials, it is assumed here that ϑ_{ut} = 0.10; that is, about 4% increase in cov above wrought steels. For cast steel materials, it taken as ϑ_{ut} = 0.08, the same value is taken for wrought nickel and wrought titanium materials. Poisson's ratio may be considered deterministic, but a cov of 0.02 [2] is suggested in critical designs. According to Ullman [51], if the material properties are well known, a cov of 0.05 may be used, if the material properties are not well known, a cov of 0.10 – 0.15 may be used. Table A1 summarizes the foregoing discussions.

Table A1: Covs for Some Strength Parameters and Materials

Strength Parameters	COV
Poisson's ratio	0.02
Wrought steel material-tensile strength	0.06
Wrought nickel material-tensile strength	0.08
Wrought titanium material-tensile strength	0.08
Cast material-tensile strength	0.10
Miscellaneous	0.05

A4.2 Fatigue Strength Variability Analysis

Based on Eq. (13), the cov for the basic approximate pulsating strength is expressed in Eq. (A6).

$$\vartheta_{so} \approx \sqrt{\vartheta_{ut}^2 + 4\vartheta_{ko}^2 + \vartheta_{\alpha e}^2 + \frac{\vartheta_{\alpha e}^2}{4}} \tag{A6}$$

From Eq. (23c), the cov for fatigue strength correction factors is expressed in Eq. (A7).

$$\vartheta_{yf} = \sqrt{\vartheta_{yn}^2 + \vartheta_{yr}^2 + \vartheta_{ys}^2 + \vartheta_{yz}^2} \tag{A7}$$

The variability in load cycles is of the other of 15% [20, p. 201] and a conservative cov of ϑ_{yn} = 0.04 may be assumed. The cov of machined surface finish is ϑ_{ys} = 0.058 [30]. The reliability factor cov is taken as ϑ_{yr} = 0.03, and the size cov is taken as ϑ_{yz} = 0.01. Hence from eq. (A7):

$$\vartheta_{yf} = \sqrt{0.04^2 + 0.03^2 + 0.058^2 + 0.01^2} = 0.077(0.08)$$

The cov for service pulsating and endurance stren–gths is a combination of the cov of the basic strengths and the cov of the effective strength correction factor of Eq. (22). The cov associated with the service approxi–mate pulsating strength is:

$$\vartheta_C = \sqrt{\vartheta_{so}^2 + \vartheta_{yf}^2} = \sqrt{0.08^2 + \vartheta_{so}^2} \tag{A8}$$

The cov for the basic accurate pulsating strength model of Eq. (11) is:

$$\vartheta_O \approx \sqrt{4\vartheta_{ut}^2 + 4\vartheta_{ko}^2 + \vartheta_{se}^2 + \frac{1}{4}\left(\vartheta_{ut}^2 + \vartheta_{se}^2\right)} \tag{A9}$$

The service accurate pulsating strength cov is:

$$\vartheta_{OC} \approx \sqrt{\vartheta_O^2 + \vartheta_{yf}^2} \qquad \vartheta_{OC} \approx \sqrt{\vartheta_O^2 + 0.08^2} \tag{A10}$$

The cov for the basic approximate endurance strength based on endurance ratio, from Eq. (10b) is obtained as:

$$\vartheta_{se} = \sqrt{\vartheta_{ut}^2 + \vartheta_{\alpha e}^2} \tag{A11}$$

For the service approximate endurance strength capability:

$$\vartheta_S = \sqrt{\vartheta_{yf}^2 + \vartheta_{se}^2} \qquad \vartheta_S = \sqrt{0.08^2 + \vartheta_{se}^2} \qquad \text{(A12)}$$

A5 Fatigue Ratios and Design Factors

The bending endurance ratio of steel is in the range of 0.4 to 0.6 [13, 14], with an average value of 0.50. The bending endurance ratio of gray cast iron is in the range of 0.4 to 0.5 [40] with 0.45 average. The bending endu–rance ratios of ferritic and pearlitic grades of ductile cast iron are similar, decreasing from 0.5 to 0.4 with increasing strength within each grade. For tempered martensite matrices, the endurance ratio decreases from 0.5 to 0.3. The average value is 0.425 for ductile cast iron [52]. Available data show that the endurance ratio of CGI ranges from 0.44 to 0.58, though values as low as 0.37 are reported [53]. The average value of endu–rance ratio for CGI is evaluated as 0.463. From data provided by Zanardi [54], the endurance ratio of ADI varies from 0.271 to 0.475 with average of 0.395. Endurance strength ratio is 0.35 for magnesium alloys, 0.25 to 0.50 for copper alloys and 0.4 [22] for bronze (0.390 average), 0.35 to 0.50 (0.425 average) for nickel alloys, 0.45 to 0.65 (0.55 average) for titanium alloys, and 0.40 for aluminum alloys [13]. Fully reversed fatigue strength data have covs in the range of 0.04 to 0.09 and a conservative value of 0.08 is commonly adopted [21] in machine design.

The load cycles for the endurance strength for magnesium, copper and nickel alloys are 10^8 and 10^7 for titanium. That for aluminum is 5×10^8 load cycles [13] and 3×10^6 load cycles for steels is assumed.

Table A2 summarizes the data discussed above and some other parameters computed from them. Columns 2, 3 and 6 in the table summarize Table A1 and the foregoing discussions on variability of fatigue ratios. Values in column 3 of Table A2 are obtained from Table A1. Entries in column 4 of Table A2 are evaluated using Eq. (A13a) with values from column 2 and 2.326, the normal variate at 99% reliability, as arguments. Entries in column 5 of the table are obtained from Eq. (13b), entries in column 6 are approximated as column 2 data range divided by the product of the mean and 6 (assuming the range is approximately equal to 6 standard deviations) because the standard deviation of the lognormal distribution is approximately equal to the cov of the normal distribution for low values of cov not more than 0.3 [49]. Entries in column 7 of the table are derived from Eq. (A6). Note that the pulsating strength covs in the last column of Table A2 are less than 0.2.

Table A3 shows results of analysis performed to obtain design factors and pulsating fatigue ratios for the materials being studied. In Table A3, the entries in column 2 are derived from Eq. (A8). The values in Column 3 of Table A3 are obtained using Eq. (18) and those of column 4 by using Eq. (19). Finally, the entries in column 5 of Table A3 are obtained from Eq. (16a).

Table A2: Fatigue Ratios of Some Materials at 50% Reliability

Material	Endurance Ratio (α_e)	Tensile Strength COV (ϑ_{ut})	Mean Strength Factor (k_o)	Pulsating Ratio (α_o)	Endurance Ratio COV ($\vartheta_{\alpha e}$)	Pulsating Ratio COV (ϑ_{so})
Gray cast iron	0.450	0.100	1.268	0.809	0.040	0.117
Ductile cast iron	0.425	0.100	1.268	0.771	0.080	0.140
Compacted graphite iron	0.463	0.100	1.268	0.827	0.060	0.127
Austempered ductile iron	0.395	0.100	1.268	0.725	0.100	0.155
Cast steel	0.450	0.080	1.208	0.801	0.040	0.100
Copper alloys	0.390	0.080	1.208	0.689	0.112	0.154
Nickel alloys	0.425	0.080	1.208	0.765	0.060	0.112
Steel and alloys	0.500	0.060	1.152	0.860	0.040	0.085
Titanium alloys	0.550	0.080	1.208	0.935	0.060	0.112
Aluminum alloys	0.400	0.080	1.208	0.728	0.020	0.092
Magnesium alloys	0.350	0.080	1.208	0.649	0.020	0.092
Average	0.448	0.087	1.229	0.801	0.066	0.122

Table A3: Nominal Pulsating Strength Factor for common Gear Materials at 99% Reliability

Material	ϑ_C	s_m	n_o	β_o
Gray cast iron	0.140	0.319	2.210	0.366
Ductile cast iron	0.160	0.328	2.263	0.341
Compacted graphite iron	0.149	0.323	2.232	0.371
Austempered ductile iron	0.173	0.335	2.303	0.315
Cast steel	0.126	0.313	2.177	0.368
Copper alloys	0.172	0.334	2.300	0.310
Nickel alloys	0.136	0.317	2.200	0.348
Steel and alloys	0.115	0.309	2.152	0.400
Titanium alloys	0.136	0.317	2.200	0.425
Aluminum alloys	0.120	0.311	2.164	0.336
Magnesium alloys	0.120	0.311	2.164	0.300
Average	0.145	0.322	2.226	0.359

Table A4: Nominal Endurance Strength Factor for common Gear Materials at 99% Reliability

Material	□$_S$	s_m	n_e	β_e
Gray cast iron	0.133	0.313	2.177	0.207
Ductile cast iron	0.150	0.321	2.220	0.191
Compacted graphite iron	0.140	0.316	2.195	0.211
Austempered ductile iron	0.161	0.326	2.252	0.175
Cast steel	0.118	0.308	2.144	0.210
Copper alloys	0.158	0.325	2.243	0.174
Nickel alloys	0.126	0.311	2.162	0.197
Steel and alloys	0.106	0.303	2.119	0.236
Titanium alloys	0.126	0.311	2.162	0.254
Aluminum alloys	0.113	0.306	2.133	0.187
Magnesium alloys	0.113	0.306	2.133	0.164
Average	0.135	0.315	2.186	0.206

From the analysis performed, the average value of the mean strength factor k_0 for tensile strength is 1.23 from the last row of column 4 in Table A2. The nominal design factor for approximate pulsating strength is n_0 = 2.23 from the last row of column 4 in Table A3. The average pulsating strength ratio is 0.359 (0.36) from the last row of column 5 of Table A3 for all the materials in the table.

For the accurate model of Eq. (11), using all data for the materials considered and based on Eq. (A10), ϑ_{OC} = 0.203. Since ϑ_M = 0.293 from Appendix A1, then from Eq. (18):

$$s_m = \sqrt{In\left[(1+0.293^2)(1+0.203^2)\right]} = 0.348$$

From Eq. (19), for z_o = 2.326 at 99% reliability:

$$n_o = \exp\left[0.348(2.326 + 0.5 \times 0.348)\right] = 2.391 \quad (2.40)$$

The values of the design factor for the approximate and accurate pulsating strength are different due to variability differences in Eq. (A6) and Eq. (A9), respectively. Because the average values for the whole data set is used for evaluating the design factors, they are generic and may be used accordingly.

A6 Nominal Endurance Strength

Table A4 shows results of similar analysis performed in Table A3 to generate design factors and endurance ratios for the material data set. From the analysis, the nominal design factor at 99% reliability for approximate endurance strength based on fatigue ratio is n_0 = 2.19 from the last row of column 4 in Table A4. The average fatigue ratio for endurance strength is 0.206 from the last row of column 5, for all the materials in the table.

The mean strength factors at 99% reliability for the endurance and pulsating strength ration can be estimated from data in Table A2. From the last row of Table A2, ϑ_{oe} = 0.66 and ϑ_{so} = 1.22. From Eq. (A13a), for β_e:

$$k_{oe} = e^{0.066(2.326+0.5\times0.066)} = 1.1865$$

Also, from Eq. (A13a), for β_o :

$$k_{op} = e^{0.122(2.326+0.5\times0.122)} = 1.338$$

From the last row of Table A2, β_e = 0.448 and β_o = 0.801. Therefore, the ratio of basic endurance strength to basic pulsating strength at 99% reliability is then:

$$\lambda_o = \frac{\beta_e}{k_{oe}} \times \frac{k_{op}}{\beta_o} = \frac{0.448}{1.1865} \times \frac{1.338}{0.801} = 0.631$$

The computation above indicates that basic endurance strength is about 63% of basic pulsating strength for most metals at 99% reliability.

A7 Reliability Factor

The nominal pulsating strength values evaluated in Table A3 are based on 99% reliability or a failure probability of 1%. Therefore, it is necessary to adjust these nominal values for other reliability values. The reliability factor is evaluated based on lognormal standard deviation of s_m = 0.322, the average value for the materials in Table A3. Table A5 gives values of the reliability factor applicable in Eq. (23) for some other reliability levels and were estimated using the method of [31]. The difference between the reliability factor values in Table A5 and those of AGMA is that the former is based on the lognormal probability density function while the latter is based on the standard normal probability distribution function [55].

A8 Mean Strength Factor

Most data available on yield and tensile strengths are quoted as minimum values. If these mechanical capabilities are treated as random variables approximated by the lognormal probability density distribution, the corresponding mean values can be estimated if the cov of the data is known. Fortunately, the cov data need not be very accurate for preliminary design. The mean value of tensile strength is given by Eq. (10a), reproduced below.

$$S_{ut}^* = k_0 S_{ut} \quad (10a)$$

The mean value factor and associated cov are evaluated from Eqs. (A13a) and (A13b), respectively [31].

$$k_0 = e^{\vartheta_{ut}(z_0+0.5\vartheta_{ut})} \qquad \vartheta_{ko} \approx z_0 \vartheta_{ut}^2 \quad (A13)$$

Minimum strength according to American Society for Testing Metals (ASTM) corresponds to 1% failure level or reliability of 99% [14, 30] which has unit normal variate z_0 = 2.326. A conservative value of ϑ_{ut} would be 0.10 from Table A1, so that $\vartheta_{ko} \approx$ 0.02 from Eq. (A13b).

Table A5: Reliability Factor for Beam Strength

Reliability Goal	Normal Variate	Reliability Factor
50	0	2.115
60	0.253	1.949
70	0.526	1.785
80	0.742	1.665
90	1.288	1.397
95	1.645	1.245
99	2.326	1.000
99.5	2.575	0.923
99.9	3.091	0.782
99.99	3.719	0.639
99.999	4.265	0.536
99.9999	4.753	0.458
99.99999	5.201	0.396

A9 Stress Interaction Factor and Variability

The value of Y_v is somewhat influenced by the comp–ressive stress in contact meshes of gears. This was ignored in the original Lewis stress model but is considered in the revised Lewis stress model of Eq. (3). Equivalent values of Y_v in modern versions of the Lewis stress model take the compressive stress into account. The stress combination factor for the virtual plane when compressive stress is neglected because it is already encapsulated in Y_v, may be expressed as in Eq. (A14) based on [23, 24].

$$k_t = \sqrt{\left(+\frac{km_n}{b}\tan\psi_b\right)^2 + 3\left[\frac{Y_v k_\tau}{\kappa k_\sigma}\right]\left(1+\tan^2\psi_b\right)} \qquad \text{(A14)}$$

The expression of Eq. (A14) contains the base helix angle which is a function of the normal pressure angle and the nominal helix angle in Eq. (1). In general, the nominal helix angle tolerance is largely dependent on applications. Typically, helix angle tolerance is ± 0.5° (±0.00873 rad.) [45]. The nominal helix angle is accurately evaluated in design computations [46]. A Japanese standard [47] specifies a maximum deviation of 40 μm over a facewidth of 4 mm for the nominal helix angle; that is a deviation of 1% for which a cov of 0.3 to 0.4% may be assumed. From the above, the no–minal helix angle is tightly controlled during manu–facturing. The normal pressure angle is held to a very tight tolerance also, perhaps better than the helix angle. Therefore, variability of the nominal helix angle and normal pressure angle may be neglected: that is, they may be considered deterministic because very small manufacturing tolerances are allowed. Similarly, the base helix angle may be considered as deterministic.

When angular parameters are treated as deterministic in Eq. (A14), then the variability analysis expression reduces to:

$$k_t = \sqrt{\left(1+\frac{km_n}{b}\right)^2 + 3\left[\frac{Y_v k_\tau}{\kappa k_\sigma}\right]^2} \qquad \text{(A15)}$$

The second term inside the square root on the right of Eq. (A15) is the main contributor to the variability of k_t. Eq. (A15) may be analyzed through functional transformations and approximation as indicated below.

$$k_t = \sqrt{Z} \qquad Z \approx 1+Y^2 \qquad \text{(A16)}$$

The cov of k_t and Z are expressed in Eqs. (A17a) and (A17b); respectively.

$$\vartheta_{kt} = 0.5\vartheta_Z \qquad \vartheta_Z \approx \frac{2Y^2\vartheta_Y}{1+Y^2} \qquad \text{(A17)}$$

Based on Eq. (A15) and Eq, (A16b), the variable Y is given by Eq. A18a and the cov of Y is given by Eq. (18b).

$$Y = \frac{\sqrt{3}k_\tau Y_v}{\kappa k_\sigma} \qquad \vartheta_Y = \sqrt{\vartheta_{k\tau}^2 + \vartheta_k^2 + \vartheta_{k\sigma}^2 + \vartheta_{Yv}^2} \qquad \text{(A18)}$$

Assuming that $\vartheta_{k\tau} \approx \vartheta_{k\sigma}$ and $\vartheta_k \approx \vartheta_{Yv}$; Eq. (A18b) becomes Eq. (A19a). The cov (ϑ_{kt}) of k_t is then approximated as in Eq. (A19b).

$$\vartheta_Y = \sqrt{2(\vartheta_{k\sigma}^2 + \vartheta_{Yv}^2)} \qquad \vartheta_{kt} \approx \frac{Y^2\vartheta_Y}{1+Y^2} \qquad \text{(A19)}$$

The parameter Y_v may be read from a graph where approximation and or reading error is unavoidable. ϑ_{Yv} is taken as 0.03. Now, $\vartheta_{k\sigma} \approx 0.11$ for shoulder fillet [30], and from Eq. (A19a):

$$\vartheta_Y = \sqrt{2(0.11^2 + 0.03^2)} = 0.161$$

Also, $k_\tau = 2.0$ [23], $Y_v = 0.4878$, $\kappa = 2.313$ [24], and $k_\sigma = 1.4$ [25]. Therefore; from Eq. A(18a):

$$Y = \frac{\sqrt{3}k_\tau Y_v}{\kappa k_\sigma} = \frac{\sqrt{3}\times 2\times 0.4878}{2.313\times 1.4} = 0.522$$

From Eq. (A19b):

$$\vartheta_{kt} \approx \frac{0.522^2\times 0.161}{1+0.522^2} = 0.0345$$

The parameter Y_t and its cov are expressed in Eqs. (A5a) and (A5b), respectively. Substituting values in Eq. (A5b):

$$\vartheta_{Yt} = \sqrt{0.03^2 + 0.0345^2} = 0.046\ (0.05)$$

Because of the computational simplification and neglected tolerances on angular parameters in the analysis, the cov of ϑ_{Yt} will be taken as 0.05.

ПРОЦЕНА ЧВРСТОЋЕ СНОПА МАТЕРИЈАЛА МЕТАЛНОГ ЗУПЧАНИКА

Е. Осакуе, Л. Анетор

Изрази за пулсирајућу снагу или јачину снопа многих популарних металних материјала зупчаника су изведени на основу затезне чврстоће и односа издржљивости. Предвиђене вредности чврстоће су

за поузданост од 99% при циклусима оптерећења која одговарају издржљивости материјала. Изрази су засновани на разматрању ревидиране формуле напрезања корена Левис-а зупчаника третирањем пројектних параметара као случајних променљивих повезаних са логнормалном функцијом густине вероватноће и применом Герберовог правила отказа замора. Предвиђања пулсирајуће јачине су упоређена са онима из АГМА процене за кроз каљене челике и друге материјале. Одступања између предвиђања модела и АГМА вредности за материјале од челика и дуктилног ливеног гвожђа су релативно ниске. Такође су примећене ниске варијације између вредности модела и АГМА за сиви ливени гвожђе високе чврстоће и ливену бронзу. Међутим, нађене су велике варијације између вредности модела и АГМА за сиви ливени гвожђе мале чврстоће и ливену бронзу. Све у свему, процене модела се сматрају довољно тачним за апликације прелиминарног дизајна где се генеришу почетне величине зупчаника. Студија је показала да је за многе металне материјале зупчаника просечан однос пулсирајуће чврстоће 0,36 уз поузданост од 99%. Стога је оправдана сугестија Буцкингхама да је заморна чврстоћа зуба зупчаника приближно једна трећина (0,333) затезне чврстоће материјала.